

Review

# Porous Zirconia Blocks for Bone Repair: An Integrative Review on Biological and Mechanical Outcomes

Cláudia Inês Resende-Gonçalves<sup>1</sup>, Nuno Sampaio<sup>1</sup>, Joaquim Moreira<sup>1</sup>, Oscar Carvalho<sup>2,3</sup> , João Caramês<sup>4</sup> , Maria Cristina Manzaneres-Céspedes<sup>5</sup> , Filipe Silva<sup>2,3</sup>, Bruno Henriques<sup>2,3,6,\*</sup> and Júlio Souza<sup>1,2,3,\*</sup> 

- <sup>1</sup> School of Dentistry, University Institute of Health Sciences (IUCS), Cooperativa de Ensino Superior Politécnico e Universitário (CESPU), 4585-116 Gandra PRD, Portugal; a23439@alunos.cespu.pt (C.I.R.-G.); nuno.sampaio@iucs.cespu.pt (N.S.); joaquim-moreira@iucs.cespu.pt (J.M.)
- <sup>2</sup> Center for Micro ElectroMechanical Systems (CMEMS-UMINHO), University of Minho, 4710-057 Braga, Portugal; oscar.carvalho@gmail.com (O.C.); fsamuel@dem.uminho.pt (F.S.)
- <sup>3</sup> Associate Laboratory (LABBELS), University of Minho, 4800-058 Guimarães, Portugal
- <sup>4</sup> Bone Physiology Research Group, LIBPhys, School of Dentistry, Universidade de Lisboa, 1600-277 Lisbon, Portugal; carames@campus.ul.pt
- <sup>5</sup> Human Anatomy and Embryology Unit, Department of Pathology and Experimental Therapy, Faculty of Dentistry, University of Barcelona, 08007 Barcelona, Spain; mcmanzaneres@ub.edu
- <sup>6</sup> Ceramic and Composite Materials Research Group (CERMAT), Department of Mechanical Engineering (EMC), Campus Trindade, Federal University of Santa Catarina (UFSC), Florianópolis 88040-900, Brazil
- \* Correspondence: brunohenriques@dem.uminho.pt (B.H.); jsouza@dem.uminho.pt (J.S.)



**Citation:** Resende-Gonçalves, C.I.; Sampaio, N.; Moreira, J.; Carvalho, O.; Caramês, J.; Manzaneres-Céspedes, M.C.; Silva, F.; Henriques, B.; Souza, J. Porous Zirconia Blocks for Bone Repair: An Integrative Review on Biological and Mechanical Outcomes. *Ceramics* **2022**, *5*, 161–172. <https://doi.org/10.3390/ceramics5010014>

Academic Editors: Gilbert Fantozzi and Enrico Bernardo

Received: 14 January 2022

Accepted: 22 February 2022

Published: 17 March 2022

**Publisher's Note:** MDPI stays neutral with regard to jurisdictional claims in published maps and institutional affiliations.



**Copyright:** © 2022 by the authors. Licensee MDPI, Basel, Switzerland. This article is an open access article distributed under the terms and conditions of the Creative Commons Attribution (CC BY) license (<https://creativecommons.org/licenses/by/4.0/>).

**Abstract:** The aim of this study was to conduct an integrative review of the biological and mechanical outcomes of porous zirconia structures for extensive bone repair. An electronic search was performed on the PubMed database using a combination of the following scientific terms: porous, scaffold, foam, zirconia, bone regeneration, bone repair, bone healing. Articles published in the English language up to December 2021 and related to porosity, pore interconnectivity, biocompatibility and strength of the material, and the manufacturing methods of zirconia porous structures were included. Randomized controlled trials and prospective cohort studies were also evaluated. The research identified 145 studies, of which 23 were considered relevant. A high percentage of pores and the size and interconnectivity of pores are key factors for cell migration, attachment, proliferation, and differentiation. In addition, pore interconnectivity allows for the exchange of nutrients between cells and formation of blood vessels. However, a decrease in strength of the porous structures was noted with an increase in the number and size of pores. Therefore, yttria-stabilized zirconia tetragonal polycrystal (Y-TZP) has mechanical properties that make it suitable for the manufacture of highly porous structures or implants for extensive bone repair. Additionally, the porous structures can be coated with bioactive ceramics to enhance the cell response and bone ingrowth without compromising pore networking. Porous structures and mesh implants composed of zirconia have become a strategy for extensive bone repair since the material and the pore network provide the desired biological response and bone volume maintenance.

**Keywords:** porous; scaffold; implant; zirconia; bone repair

## 1. Introduction

Although many biomedical materials have been suggested for bone-healing and tissue-engineering applications, bioactivity, design and physical properties are still clinical limitations of current scaffolds and porous implants [1–3]. In fact, scaffolds and porous implants should have the following criteria for enhanced bone healing: high cytocompatibility for cell migration and differentiation, appropriate mechanical properties to support loading, and interconnected porosity to allow cell migration and nutrients exchange [4–7]. Porosity, pore size and even pore interconnectivity significantly affect cell behavior, angiogenesis,

and bone ingrowth in porous ceramics [5,7,8]. Effective flowing and transportation of nutrients through the pores enable bone-tissue growth whereas the increased surface area of porous structures leads to better bonding with host tissues [9,10]. However, a high porosity and the pore size of the scaffold or porous implant affect their mechanical properties.

Bioactive ceramics composed of calcium and phosphates are the first choice as a source material for bone reconstructive scaffolds due to their bioactivity and bone-healing stimuli. However, the mechanical properties of current bioactive materials are not appropriate for repair of extensive bone defects [3,9,11–13]. For instance, the compressive strength of pure hydroxyapatite porous blocks is low (~0.3 MPa) when compared to trabecular (~12 MPa) or cortical bone (~200 MPa) [14,15]. A scaffold or porous implant should withstand loading during handling and surgical procedures for periodontal and peri-implant therapies. In cases of extensive bone loss, the endosseous porous structure must possess mechanical properties to avoid fractures from occlusal stresses that could compromise the bone ingrowth process [2,3]. A balance between the desired mechanical and biological functions can be established by controlling the porosity and selection of biocompatible ceramics [7,9,13].

In this way, biocompatible materials composed of zirconia with desired properties such as strength, fracture toughness, chemical stability, and high biocompatibility have been designed for biomedical applications [6,16–22]. In medicine, zirconia has been used for orthopedic implants and prostheses [7,20,23–25]. In the field of dentistry, zirconia can be used for dental implants and prosthetic structures such as crowns and on-lay, in-lay, and multi-unit prostheses [16,21,26–31]. In addition, particulate zirconia can be used as a micro- or nano-scale filler in hybrid resin–matrix composites [18,26,31]. The use of zirconia fillers has significantly increased the mechanical properties of hybrid resin–matrix composites [26,31]. Zirconium dioxide ( $ZrO_2$ ), known as zirconia, adopts a tetragonal structure at high temperature between 1170 and 2370 °C and a monoclinic crystal at room temperature. In vitro and in vivo studies have consistently shown that zirconia, in its various physical forms (monoclinic, cubic, or tetragonal phase) [32,33]. Zirconium dioxide is often doped with metal oxides such as yttria ( $Y_2O_3$ ), magnesium oxide (MgO), or calcium oxide (CaO), to stabilize tetragonal phase [33,34]. Yttria-stabilized zirconia polycrystals (Y-TZP) have an elastic modulus of 240–270 GPa, a flexural strength of 1200 MPa, a fracture toughness of 8  $MPa \cdot m^{1/2}$ , and a high biocompatibility [13,33–35]. The load-bearing capability of Y-TZP is important in maintaining bone volume and avoiding continuous tissue remodeling after placement of a porous structure. Zirconia (Y-TZP) porous structures can achieve a compressive strength ranging from 5 to 10 MPa that is crucial for clinical handling and clinical success over the period required for bone healing [7,13–15,36,37]. Additionally, bioactive ceramics are used to cover the porous structures for enhanced cell stimulation while maintaining the porosity [5,7,36,38,39]. Porous zirconia structures have been manufactured and coated with bioactive ceramics such as calcium-phosphate-based ceramics [5,6,11,32,40]. In an in vivo study, porous zirconia was used as a substrate for hydroxyapatite (Hap) coating, resulting in a strong and bioactive porous structure to stimulate bone repair. In fact, zirconia enhanced the overall osteoconductivity of the porous structure and improved its mechanical properties while the bioactive coating improved the bone ingrowth [5,7,10,40]. Hydroxyapatite coatings or scaffolds form an apatite outer layer which they chemically react with proteins, blood platelets, or osteogenic cells [6,41–45]. Proteins and minerals also interact with zirconia leading to the activation of blood platelets and migration of osteogenic cells [21,32,35,43,46].

The main aim of this study was to perform an integrative review on the mechanical and biological beneficial effects of zirconia porous structures or mesh implants for extensive bone repair. It was hypothesized that a balanced porosity and pore size in porous zirconia structures enhance the osteogenic cell behavior, angiogenesis, and bone formation.

## 2. Materials and Methods

### 2.1. Information Sources and Search Strategy

A literature search was performed on PubMed (via National Library of Medicine) as this database includes major articles in the field of dentistry and biomaterials. The search was performed in accordance with the search strategy applied in previous studies on integrative or systematic reviews [21,47–54]. The following combination of search terms was applied: “porous” OR “scaffold” OR “foam” AND “zirconia” OR “bone regeneration” OR “bone repair” OR “bone healing”. The inclusion criteria encompassed articles published in the English language, until 26 December 2021, that reported the effect of porous zirconia structures on osteoblast growth and bone repair. The eligibility inclusion criteria used for article searches also included articles written in English, in vitro testing, meta-analyses, randomized controlled trials, animal assays, and prospective cohort studies. The exclusion criteria were as follows: papers without an abstract, case reports with a short follow-up period, and porous zirconia for non-biomedical applications. In addition, a hand-search was performed on the reference lists of all primary sources and eligible studies of this integrative review for additional relevant publications. Studies based on publication date were not restricted during the search process.

### 2.2. Study Selection and Data Collection Process

The articles retrieved by the search process were evaluated in three steps. On Mendeley citation manager (Elsevier B.V., Amsterdam, The Netherlands), the articles were compiled for each combination of key terms and therefore duplicates were removed. Studies were primarily scanned for relevance by title and the abstracts of those not excluded at this stage were assessed. The second step comprised the evaluation of the abstracts and non-excluded articles, according to the eligibility criteria of the abstract review. Three of the authors (J.S., C.I.R.-G., and N.S.) independently evaluated the titles and abstracts of potentially pertinent articles. An initial evaluation of the abstracts was carried out to establish whether the articles met the main aim of the study. Selected articles were individually read and analyzed according to the purpose of this study. Finally, the eligible articles received a study nomenclature label, combining first author names and year of publication. Two reviewers independently collected and catalogued data such as authors' names, journal, publication year, objectives, zirconia preparation, zirconia type, porosity, pore size and interconnectivity, bone growth, osteoblast proliferation, and osteoblast viability. Data of the reports were harvested directly into a specific data-collection form to avoid multiple data recording from more than one report within the same study (e.g., reports with different set-ups). This evaluation was individually carried out by two researchers, followed by a joint discussion to select the relevant studies.

## 3. Results

The literature search identified a total of 145 articles in PubMed, as shown in Figure 1. After reading the titles and abstracts of the articles, 92 were excluded because they did not meet the inclusion criteria. The remaining 27 potentially relevant studies were then evaluated (Figure 1). Of those articles, 4 studies were excluded because they did not contain comprehensive data related to the purpose of the present study. Thus, 23 studies were included in this review. Of the 23 selected studies, 3 (13%) articles investigated the surface topography, 11 (47.8%) evaluated the biocompatibility, 7 articles (30.4%) evaluated the effect of porosity, and 2 (8.7%) articles investigated the environmental degradation and its influence on mechanical properties. The main outcomes of the selected studies were as follows:

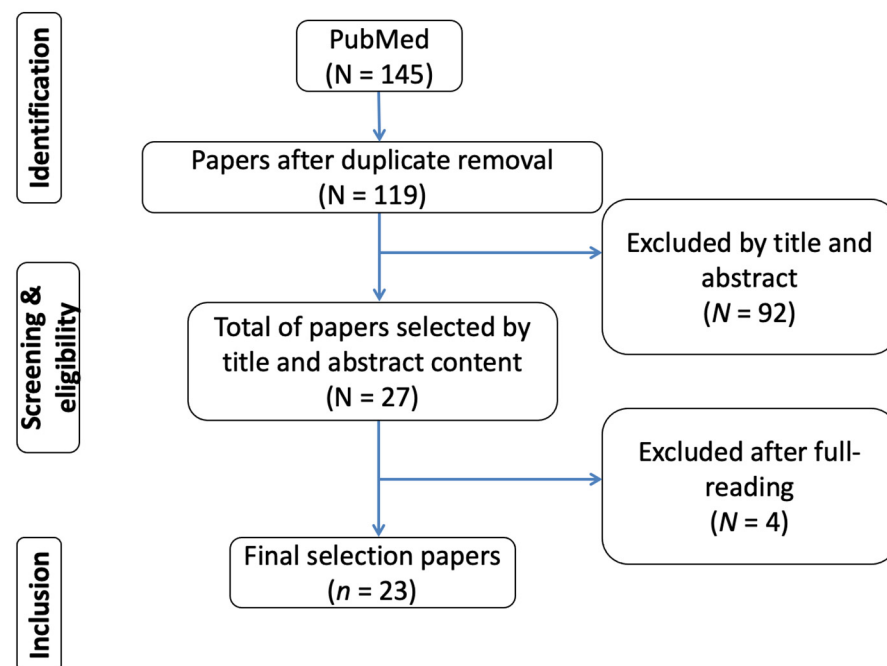


**Figure 1.** Flow diagram of the search strategy used in this study.

Most of the studies assessed zirconium dioxide (zirconia) containing 3%  $Y_2O_3$ , known as Y-TZP, which has a high strength and biocompatibility (Supplementary Materials Table S1). Y-TZP have been used in implants although there are a few studies on the effect of the porosity on the mechanical properties [10,55]; A porosity above 70% is beneficial to osteogenic differentiation and therefore a macro-scale pore size ranging from 100 to 400  $\mu m$  promotes cell ingrowth and angiogenesis into the porous structure [1,2,9,11,12,15,32,40,41,56–58]. In addition, the size of the pores enhances the transfer of nutrients and oxygen between the cells. Pores at macro-scale (1–50  $\mu m$ ) provide an increase in the wettability of the porous structure as well as in the adhesion of proteins and cells [7,11,57]. Blood fluid flow, cell migration, and angiogenesis also depend also on the interconnectivity between the pores at different macro- and micro-scales thereby establishing a 3D vascular network [5,7,11,57,59]. Results revealed a high pores' interconnectivity rate linked to a high porosity [14,32]. On osteoblast growth, cells adhere to surfaces and spread into the interconnected pores [7–10,56]. Viability, proliferation, and differentiation of cells increase when the porosity and pore size increases [8–10,32,56]. Some studies showed that cell adhesion changed depending on the chemical composition of the zirconia. Porous structures containing more than 80%  $ZrO_2$  showed less affinity to cells than those containing less  $ZrO_2$  [14]. Zirconia porous structures with Hap significantly enhanced cell proliferation [2,11,12,15]. In vivo studies reported a faster bone formation into porous structures with a higher porosity and enriched with Hap [1,2,12,40]. New bone ingrowth started by lining the surfaces and gradually filling the entire pore volume from the periphery of the porous structures towards the core. Radiographic examination showed clear boundaries of surrounding bone to zirconia interfaces. After healing time, the bone to zirconia porous region reveals a transition zone due to the gradual deposition and ingrowth of bone tissue [11,12].

#### 4. Discussion

The present integrative review reports the major results of relevant previous studies taking into account the effect of the zirconia porous structures on cell migration and differentiation, angiogenesis, and bone formation. Macro-scale pores size ranging from 100 to 400  $\mu m$  allow cell ingrowth and angiogenesis into the porous structures, while pores at micro-scale (1–50  $\mu m$ ) provide an increase in wettability, protein adsorption, and cell adhesion. Considering the mechanical behavior, a high zirconia porosity at approximately

85% and large pores ranging from 100 to 400  $\mu\text{m}$  can be accomplished without compromising the application of zirconia porous structures in extensive surgical bone sites. Thus, the findings validate the hypothesis of this study. A detailed discussion of the main biological and mechanical benefits of zirconia porous structures for bone healing follows.

#### 4.1. Zirconia

Zirconia is a ceramic that has been introduced in the biomedical field for replacing metallic materials mainly due its high biocompatibility and mechanical properties [21,33–35]. In the last decade, yttria-stabilized tetragonal zirconia polycrystals (Y-TZP) have emerged in dentistry as a promising material for several applications such as single- and multi-unit restorative structures due to aesthetic outcomes such as color and opacity that mimic the natural tooth appearance [16,21,33–35,49]. The flexural strength of YTZP is around 900–1200 MPa [13,32–34,37] while the fracture toughness is approximately 6 MPa [13,32–34,37]. Nevertheless, monolithic zirconia has some limitations for endosseous implants linked to its high elastic modulus (at about 240–260 GPa) and ultralow chemical reactivity for osteogenic cell stimulation. The elastic modulus of zirconia is significantly higher than that recorded on cortical bone (10–20 GPa), which can result in stress-shielding and peri-implant bone loss [13,16,23,33,60,61].

Zirconia can be found in three polymorphic forms at ambient pressure—monoclinic up to 1170 °C, tetragonal between 1170 and 2370 °C, and cubic between 2370 and 2706 °C [33,34]. Zirconium dioxide ( $\text{ZrO}_2$ ) adopts a tetragonal structure at usual sintering temperature and a monoclinic crystal after cooling down to the room temperature. The volume expansion caused by cooling from high temperature results in crack propagation. Then, yttrium oxide ( $\text{Y}_2\text{O}_3$ ), magnesium oxide (MgO), or calcium oxide (CaO) has been added to the  $\text{ZrO}_2$  to retain the tetragonal phase and synthesize the YTZP [33,34]. Y-TZP has shown proper biocompatibility and mechanical properties in comparison to other TZPs [56,57]. MgO-stabilized zirconia also exhibits high mechanical strength, excellent chemical stability, and adequate biocompatibility [10].

Suitable elastic modulus and the wettability of zirconia can be achieved with the manufacture of zirconia porous structures [13,20,36]. A highly porous zirconia (~85%) still maintains a high compressive strength of around 5–10 MPa [2,15]. Biocompatible ceramic scaffolds support in vitro and in vivo cell growth although the mechanical properties for extensive bone repair are still a challenge. Another challenge deals with the modelling of complex structures to accurately build up their microstructural design [62]. Bioactive scaffolds composed of calcium-based structures (e.g., hydroxyapatite) provide very limited control over the inner architecture of the material and consequently have low strength [1,3,5]. Scaffolds are further required to have a suitable design that can promote the entire infiltration of bone tissue and blood vessels as occurs when autograft and allografts are used.

The 3D open cell structures show the most interesting design for bone tissue engineering applications due to their similar structure to the trabecular bone. For instance, the spongy shape of the trabecular bone can be acquired via the replica method in the manufacturing of  $\text{ZrO}_2$  foams with different porous design [7,62]. Recent developments in computer-aided design (CAD) and rapid prototyping methods have become a feasible solution since the 3D design can be carefully planned at macro- and micro-scale prior to the manufacturing of porous structures or mesh implants [12,13,62]. Free-form fabrication, which uses a 3D-printing principle, is an effective method for controlling pore architecture (size, shape and interconnectivity) of the porous structures for specific clinical applications [8,62]. Previous experimental studies on the bone response to different ceramic materials have shown results revealing not only the material effects but also the effect of the 3D design on the biological and mechanical response of the scaffolds or mesh implants [1,7,8,10,40,56].

#### 4.2. Manufacturing of Zirconia Porous Structures

Porous zirconia can be produced by different methods such as powder sintering, CAD-CAM, and the replica method, as illustrated in Figure 2. In the replica method, a polyurethane foam template with proper dimensions is impregnated with the ceramic slurry [2,7,32]. The zirconia slurry mixture is often prepared by ultrasonic dispersion into distilled water. Then, the polyurethane template is immersed in the slurry and centrifuged to remove excessive ceramic slurry. After drying at 80 °C for 12 h, zirconia is thermally treated at 800 °C for 1 h and then at 1350 °C for 5 h at a heating rate of 2 °C min<sup>-1</sup> before cooling to room temperature [32]. A previous study evaluated the effect of several thermal treatment (one, three, five, or seven) on the morphological aspects of the zirconia porous structures. The porous structure and porosity of the zirconia were affected by the sintering cycles [32]. As the number of sintering cycles increased, the pore size and porosity decreased. Porosity decreased from 92 down to 68 % when the sintering cycles increased from one to seven, at an average rate of decrease in porosity of about 4% per sintering cycle. Specimens with a higher porosity had well inter-connected pores although specimens with lower porosity had pores with limited interconnectivity. Clogged pores appeared in the porous structures treated with five sintering cycles and were apparent in porous structures treated with seven sintering cycles. The compressive strength of the zirconia porous structures increased from 0.6 to 4.4 MPa when the sintering cycles were increased from one to seven and, correspondingly, the porosity of the zirconia decreased from 92 to 68% [32].

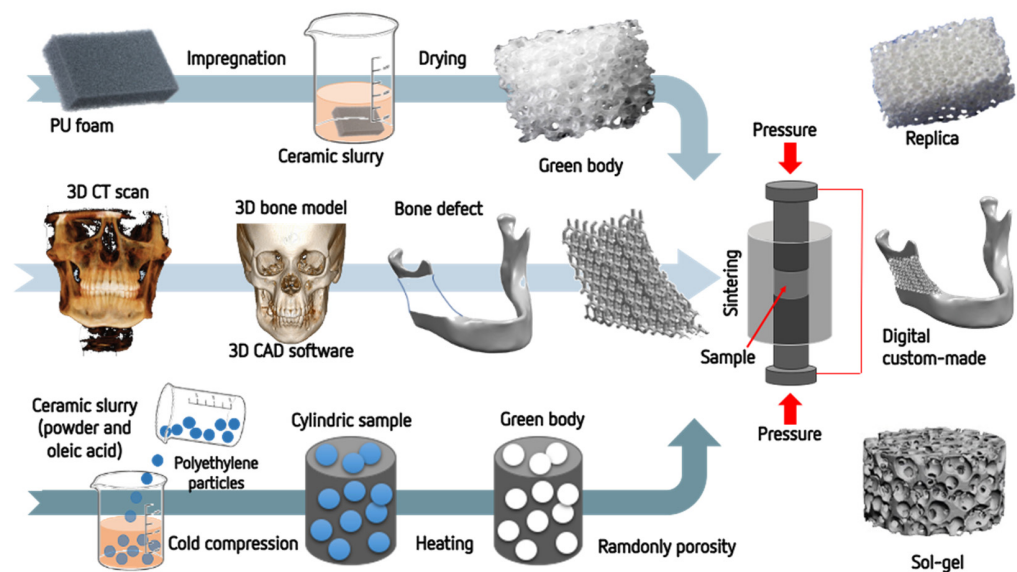


**Figure 2.** Schematics of the porous zirconia manufacturing.

In another study, the pores' size was controlled by utilizing two types of polyurethane foam templates with 45 ppi for acquiring large pores and 60 ppi for small pores. In addition, the porosity was controlled at approximately 75 or 85% by adjusting the replication cycle. Spherical pores with size of around 500–700 µm and 150–200 µm were detected. Pores were well-interconnected, without showing any pore-blockings. However, some pores were severely clogged in the specimens with low porosity. As expected, the compressive strength was lower in porous structures with higher porosity [2].

The zirconia powder can be milled to produce different dimensions of zirconia particles or a mixture of zirconia and other oxides. A previous study assessed the effect of a mixture of zirconia and alumina on the porosity and mechanical properties of zirconia- and alumina-based porous structures [9]. The ceramic powders were submitted to ball milling for 25 h to reduce agglomeration and heterogeneity of the powder. Ceramic slurries were produced from different ceramic powders mixed with oleic acid as dispersant. Macro-

particle polyethylene particles of 90–250  $\mu\text{m}$  and 20 vol% were placed into the ceramic slurries as macro-pore formers during the thermal treatment [9]. Polyethylene particles were eliminated by thermal treatment at 300 °C for 3 h (heating rate of 200 °C/h) in an air furnace. The pores were maintained after thermal treatment and cooling down at room temperature [9,10]. The mixtures were hydraulically pressed on 100 MPa in steel die molds to produce cylindrical (15 mm diameter, 5 mm height) specimens [9,10]. On thermal treatment, the organic material was removed, generating the desired pores within the microstructure. Sintering was performed at 1400 °C in LHT 02/17 high-temperature furnaces (Nabertherm, Germany) in air environment over an isothermal exposure time of 2 h [9]. During the sintering process, the percentage of shrinkage cannot be controlled and therefore small dimensional variations can take place [9].

Regarding the CAD-CAM method, zirconia porous structures can be designed by CAD (e.g., STL file) for further manufacturing processes. In this way, the porous structures are manufactured with different dimensions, porosity, pores' networking, and size of pores [14,21,22]. The percentage of shrinkage can be estimated in order to control the dimensions of porous structures and pores after thermal treatment [57]. The manufacturing process can involve 3D-printing or micro-machining processes. A thermoplastic polymeric material can be used as a molding structure, surrounded by a holding wax-based material. The holding material are detached from the mold leading to the building up of the struts and pores of the zirconia [1,8]. The molds are infiltrated with 50 vol% zirconia slurries prepared by the ball-milling process. The ceramic suspensions can be accomplished by using slip casting (colloidal filtration) in which the excess of water is drained from the suspension on a plaster plate [1,8]. The use of colloidal slip-casting processes provides a variety of zirconia structures depending on the percentage and size of pores [5,7,57]. In a previous study, zirconia/hydroxiapatite (Hap) assemblies were heated to 600 °C at 1 °C/min to burn away the mold and additives. Further heating on Hap was performed at 5 °C/min up to 1200 °C and on zirconia at 5 °C/min up to 1500 °C for 2 h. The mean pore size of the sintered materials was recorded at approximately 1.2  $\mu\text{m}$  and 390 nm for Hap and zirconia porous structures, respectively [8]. The macro-scale porosity of approximately 40 vol% consisted of square-shaped and interconnected pore channels with a mean size of approximately 350  $\mu\text{m}$  [1,57].

#### 4.3. Biological Effects of Porous Zirconia Structures

The size, percentage, and interconnectivity of pores are critical morphological properties influencing the biological efficiency of the porous structures, as shown in Table S1. Previous studies reported that high porosity and large pore size at macro-scale (100–400  $\mu\text{m}$ ) induce migration, adhesion, and differentiation of osteogenic cells as well as angiogenesis, nutrient exchange, and bone formation [2,7,10–12,40,56]. It should be emphasized that the formation of the vessels' network (angiogenesis) needs to occur prior to bone in-growth [8,63]. However, the size of pores can decrease the strength of the porous structures. Interconnectivity, which is related to both pore size and the extent of porosity is required to promote body fluid stream [32] and cell migration to the core of the implant, as illustrated in Figure 3. Several reports in the literature emphasizes the importance and benefits of pores' interconnectivity on bone growth and implant fixation [15,26,42]. A recent study attributed enhanced cell viability to the internal porous structure rather than to the type of struts and bioactive coating material [12]. Another morphological study reported that the coated porous structure was partially filled as compared to the non-coated zirconia structure. The filling of a porous structure decreases the internal porous network. Porous structures with a higher porosity should also reveal well-interconnected pores although the strength and surgical handling of the porous structures must be preserved [14,32].

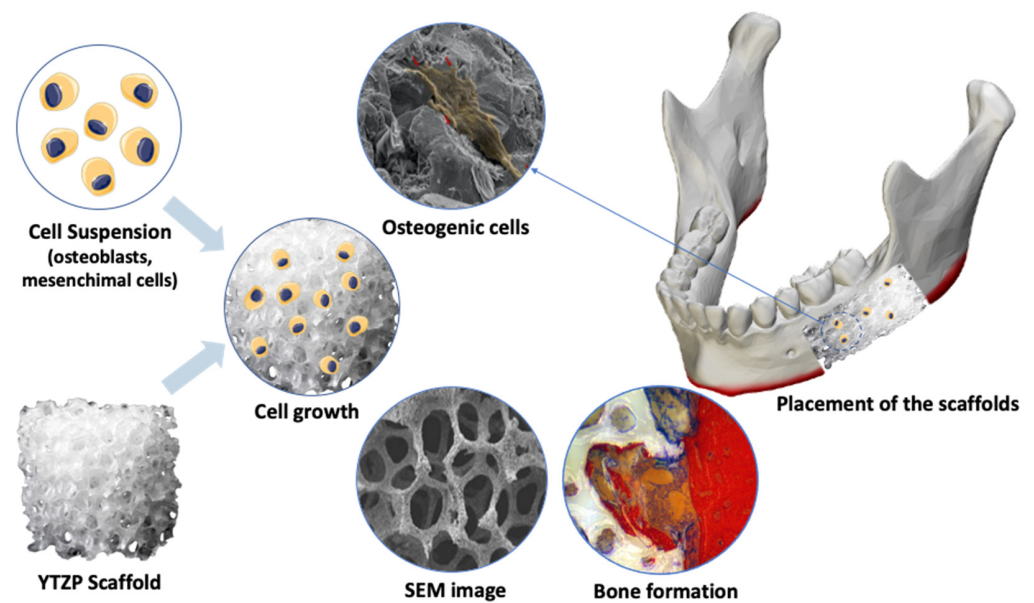


**Figure 3.** Schematics of the cell growth in the porous zirconia structures.

Although porous structures with a higher porosity are suggested to be more desirable with respect to bone-formation capability, mechanical benefits resulting from the decrease in porosity should not be ignored. The mechanical performance of porous structures is crucial for bone repair in the case of extensive bone loss such as defects of the jaw body or ramus [2,13,32]. Thus, a balance of porosity and strength must be accomplished for enhanced bone healing [3,7,13]. For the growth of osteogenic cells, porous surfaces support the adhesion and spreading of the cells from the outer region throughout the pore network [5,7,10,56]. A larger number of cells with size between 100–400  $\mu\text{m}$  can proliferate into pores due to the surface area for attachment and space for nutrient exchange [58].

A recent study reported optimum conditions for cell growth, proliferation, and extracellular cell matrix (ECM) when the specimen porosity was approximately at 90% [15]. A higher number of cells was detected on specimens with higher porosity (~93%) when compared to porous structures with 68% porosity [32]. Previous studies had validated that pores with diameter larger than 100  $\mu\text{m}$  can provide a proper framework for the proliferation, differentiation, and migration of osteoblast, chondrocyte, and vascular endothelial cells [40]. Additionally, the cell behavior inside an endosseous porous structures is also influenced by the effect of the material chemistry as occurs on zirconia-coated porous structures with bioactive ceramics [1]. New bone growth starts by lining and gradually filling the entire pore volume [2,11,12,40].

In vivo studies have also shown the beneficial effects of the higher porosity on the osseointegration events, as illustrated in Figure 3. A previous study in rabbit calvaria bone defects reported that porous structures with high porosity percentages (84–87%) and high pores' interconnectivity exhibit significantly higher bone formation when compared to the porous structures with a lower porosity (75%). A previous study on tibia and femur of rabbits reported that the areas inside the porous structures were filled with irregular woven bone [2]. Blood vessels were detected in the newly formed bone inside the macro-scale pores. In addition, irregular woven bone was noticed as bone trabeculae reaching the porous structures from the surrounding bone. Bone tissue was often found in intimate contact with the surfaces of porous structures in both the outer and inner regions [1,2]. Another study had found that new bone tissue of 2–3 mm depth had grown into the porous structures within three months of surgical placement [40]. The pores of the specimens were entirely filled with new bone tissue within 12 months without any clinical issues [40]. In addition, such findings also showed that the porous materials had improved mechanical properties and biocompatibility [40].

## 5. Conclusions

In the present review, relevant articles reported significant biological and physical evidence of the effect of zirconia porous structures for enhanced bone healing. The main outcomes of the selected studies were as follow:

- Most studies described the manufacturing of zirconia porous structures by using CAD-CAM, replica methods, and powder sintering. Control of the size and percentage of pores can be achieved by designing the models by CAD or polyurethane patterns;
- Considering the mechanical properties of zirconia, a high porosity of approximately 85% and large pores ranging from 100 up to 400  $\mu\text{m}$  can be accomplished without compromising the application of zirconia porous structures in extensive surgical bone sites;
- Macro-scale pores ranging from 100 to 400  $\mu\text{m}$  allow cell ingrowth and angiogenesis into the porous structures, while pores at micro-scale (1–50  $\mu\text{m}$ ) provide an increase in the wettability, protein adsorption, and cell adhesion;
- Most in vivo studies reported increased bone growth by contact and distance osteogenesis into the porous zirconia compared to highly dense zirconia. Porous zirconia showed significantly improved new bone formation into the interconnected channels after placement in rabbits for 4 and 12 weeks and after placement in humans for about 3 months;
- Further studies should be carried out to determine the optimum balance between porosity, pores' size, and the strength of the porous zirconia structures. In addition, hybrid bioactive ceramic containing zirconia and modified surfaces could be explored as the surfaces of porous structures play a key role in the adsorption of proteins and osteogenic cells.

**Supplementary Materials:** The following supporting information can be downloaded at: <https://www.mdpi.com/article/10.3390/ceramics5010014/s1>, Table S1: Data from the selected studies.

**Author Contributions:** Conceptualization, J.S., J.M. and N.S.; methodology, N.S., C.I.R.-G., J.S. and O.C.; investigation, J.S., N.S. and C.I.R.-G.; writing—original draft preparation, J.S., N.S., C.I.R.-G., B.H., J.C. and F.S.; writing—review and editing, J.S., B.H., M.C.M.-C. and J.M.; supervision, F.S., J.C. and J.S. All authors have read and agreed to the published version of the manuscript.

**Funding:** This study was supported by the following FCT projects (Portugal): UID/EEA/04436/2013, POCI-01-0145-FEDER-031035\_LaserMULTICER, SFRH/BPD/123769/2016, and LIBPhys-FCT UID/FIS/04559/2013. Also, it was supported by the following CNPq project (Brazil): CNPq/UNIVERSAL/421229/2018-7.

**Data Availability Statement:** Not applicable.

**Conflicts of Interest:** The authors declare no conflict of interest.

## References

1. Malmstrom, J.; Adolfsson, E.; Emanuelsson, L.; Thomsen, P. Bone ingrowth in zirconia and hydroxyapatite scaffolds with identical macroporosity. *J. Mater. Sci. Mater. Med.* **2008**, *19*, 2983–2992. [[CrossRef](#)] [[PubMed](#)]
2. Kim, H.-W.; Shin, S.-Y.; Kim, H.-E.; Lee, Y.-M.; Chung, C.-P.; Lee, H.-H.; Rhyu, I.-C. Bone formation on the apatite-coated zirconia porous scaffolds within a rabbit calvarial defect. *J. Biomater. Appl.* **2008**, *22*, 485–504. [[CrossRef](#)] [[PubMed](#)]
3. Deschamps, I.S.; Magrin, G.L.; Magini, R.S.; Fredel, M.C.; Benfatti, C.A.M.; Souza, J.C.M. On the synthesis and characterization of  $\beta$ -tricalcium phosphate scaffolds coated with collagen or poly (D, L-lactic acid) for alveolar bone augmentation. *Eur. J. Dent.* **2017**, *11*, 496–502. [[CrossRef](#)] [[PubMed](#)]
4. Bhowmick, A.; Pramanik, N.; Jana, P.; Mitra, T.; Gnanamani, A.; Das, M.; Kundu, P.P. Development of bone-like zirconium oxide nanoceramic modified chitosan based porous nanocomposites for biomedical application. *Int. J. Biol. Macromol.* **2017**, *95*, 348–356. [[CrossRef](#)] [[PubMed](#)]
5. Mesquita-Guimarães, J.; Detsch, R.; Souza, A.C.; Henriques, B.; Silva, F.S.; Boccacini, A.R.; Carvalho, O. Cell adhesion evaluation of laser-sintered HAp and 45S5 bioactive glass coatings on micro-textured zirconia surfaces using MC3T3-E1 osteoblast-like cells. *Mater. Sci. Eng. C* **2020**, *109*, 110492. [[CrossRef](#)]

6. Peñarrieta-Juanito, G.; Cruz, M.; Costa, M.; Miranda, G.; Marques, J.; Magini, R.; Mata, A.; Souza, J.C.M.; Caramês, J.; Silva, F.S. A novel gradated zirconia implant material embedding bioactive ceramics: Osteoblast behavior and physicochemical assessment. *Materialia* **2018**, *1*, 3–14. [[CrossRef](#)]
7. Gouveia, P.F.; Mesquita-Guimarães, J.; Galárraga-Vinueza, M.E.; Souza, J.C.M.; Silva, F.S.; Fredel, M.C.; Boccaccini, A.R.; Detsch, R.; Henriques, B. In-vitro mechanical and biological evaluation of novel zirconia reinforced bioglass scaffolds for bone repair. *J. Mech. Behav. Biomed. Mater.* **2021**, *114*, 104164. [[CrossRef](#)]
8. Grandfield, K.; Palmquist, A.; Ericson, F.; Malmstrom, J.; Emanuelsson, L.; Slotte, C.; Adolfsson, E.; Botton, G.A.; Thomsen, P.; Engqvist, H. Bone response to free-form fabricated hydroxyapatite and zirconia scaffolds: A transmission electron microscopy study in the human maxilla. *Clin. Implant Dent. Relat. Res.* **2012**, *14*, 461–469. [[CrossRef](#)]
9. Hadjicharalambous, C.; Buyakov, A.; Buyakova, S.; Kulkov, S.; Chatzinikolaidou, M. Porous alumina, zirconia and alumina/zirconia for bone repair: Fabrication, mechanical and in vitro biological response. *Biomed. Mater.* **2015**, *10*, 25012. [[CrossRef](#)]
10. Hadjicharalambous, C.; Mygdali, E.; Prymak, O.; Buyakov, A.; Kulkov, S.; Chatzinikolaidou, M. Proliferation and osteogenic response of MC3T3-E1 pre-osteoblastic cells on porous zirconia ceramics stabilized with magnesia or yttria. *J. Biomed. Mater. Res. A* **2015**, *103*, 3612–3624. [[CrossRef](#)]
11. Shao, R.-X.; Quan, R.-F.; Wang, T.; Du, W.-B.; Jia, G.-Y.; Wang, D.; Lv, L.-B.; Xu, C.-Y.; Wei, X.-C.; Wang, J.-F.; et al. Effects of a bone graft substitute consisting of porous gradient HA/ZrO<sub>2</sub> and gelatin/chitosan slow-release hydrogel containing BMP-2 and BMSCs on lumbar vertebral defect repair in rhesus monkey. *J. Tissue Eng. Regen. Med.* **2018**, *12*, e1813–e1825. [[CrossRef](#)] [[PubMed](#)]
12. Aboushelib, M.N.; Shawky, R. Osteogenesis ability of CAD/CAM porous zirconia scaffolds enriched with nano-hydroxyapatite particles. *Int. J. Implant Dent.* **2017**, *3*, 21. [[CrossRef](#)] [[PubMed](#)]
13. Fabris, D.; Mesquita-Guimarães, J.; Pinto, P.; Souza, J.C.M.; Fredel, M.C.; Silva, F.S.; Henriques, B. Mechanical properties of zirconia periodic open cellular structures. *Ceram. Int.* **2019**, *45*, 15799–15806. [[CrossRef](#)]
14. Alizadeh, A.; Moztarzadeh, F.; Ostad, S.N.; Azami, M.; Geramizadeh, B.; Hatam, G.; Bizari, D.; Tavangar, S.M.; Vasei, M.; Ai, J. Synthesis of calcium phosphate-zirconia scaffold and human endometrial adult stem cells for bone tissue engineering. *Artif. Cells Nanomed. Biotechnol.* **2016**, *44*, 66–73. [[CrossRef](#)] [[PubMed](#)]
15. An, S.-H.; Matsumoto, T.; Miyajima, H.; Nakahira, A.; Kim, K.-H.; Imazato, S. Porous zirconia/hydroxyapatite scaffolds for bone reconstruction. *Dent. Mater.* **2012**, *28*, 1221–1231. [[CrossRef](#)] [[PubMed](#)]
16. Pessanha-Andrade, M.; Sordi, M.B.; Henriques, B.; Silva, F.S.; Teughels, W.; Souza, J.C.M. Custom-made root-analogue zirconia implants: A scoping review on mechanical and biological benefits. *J. Biomed. Mater. Res.-Part B Appl. Biomater.* **2018**, *106*, 2888–2900. [[CrossRef](#)] [[PubMed](#)]
17. Henriques, B.; Fabris, D.; Souza, J.C.M.; Silva, F.S.; Mesquita-Guimarães, J.; Zhang, Y.; Fredel, M. Influence of interlayer design on residual thermal stresses in trilayered and graded all-ceramic restorations. *Mater. Sci. Eng. C* **2016**, *71*, 1037–1045. [[CrossRef](#)]
18. Souza, J.C.M.; Silva, J.B.; Aladim, A.; Carvalho, O.; Nascimento, R.M.; Silva, F.S.; Martinelli, A.E.; Henriques, B. Effect of Zirconia and Alumina Fillers on the Microstructure and Mechanical Strength of Dental Glass Ionomer Cements. *Open Dent. J.* **2016**, *10*, 58–68. [[CrossRef](#)] [[PubMed](#)]
19. Dantas, T.A.; Roedel, S.; Flores, P.; Mesquita-Guimarães, J.; Souza, J.C.M.; Fredel, M.C.; Silva, F.S.; Henriques, B. Wear behaviour of tetragonal zirconia polycrystal with a porous surface. *Int. J. Refract. Met. Hard Mater.* **2018**, *75*, 85–93. [[CrossRef](#)]
20. Roedel, S.; Mesquita-Guimarães, J.; Souza, J.C.M.; Silva, F.S.; Fredel, M.C.; Henriques, B. Production and characterization of zirconia structures with a porous surface. *Mater. Sci. Eng. C* **2019**, *101*, 264–273. [[CrossRef](#)]
21. Cunha, W.; Carvalho, O.; Henriques, B.; Silva, F.S.; Özcan, M.; Souza, J.C.M. Surface modification of zirconia dental implants by laser texturing. *Lasers Med. Sci.* **2022**, *37*, 77–93. [[CrossRef](#)] [[PubMed](#)]
22. Henriques, B.; Fabris, D.; Souza, J.C.M.; Silva, F.S.; Carvalho, Ó.; Fredel, M.C.; Mesquita-Guimarães, J. Bond strength enhancement of zirconia-porcelain interfaces via Nd:YAG laser surface structuring. *J. Mech. Behav. Biomed. Mater.* **2018**, *81*, 161–167. [[CrossRef](#)] [[PubMed](#)]
23. Chen, Y.-W.; Moussi, J.; Drury, J.L.; Wataha, J.C. Zirconia in biomedical applications. *Expert Rev. Med. Devices* **2016**, *13*, 945–963. [[CrossRef](#)] [[PubMed](#)]
24. Gremillard, L.; Martin, L.; Zych, L.; Crosnier, E.; Chevalier, J.; Charbouillot, A.; Sainsot, P.; Espinouse, J.; Aurelle, J.-L. Combining ageing and wear to assess the durability of zirconia-based ceramic heads for total hip arthroplasty. *Acta Biomater.* **2013**, *9*, 7545–7555. [[CrossRef](#)] [[PubMed](#)]
25. Kim, Y.-H.; Kim, J.-S. Tribological and material analyses of retrieved alumina and zirconia ceramic heads correlated with polyethylene wear after total hip replacement. *J. Bone Jt. Surg. Br.* **2008**, *90*, 731–737. [[CrossRef](#)]
26. Rodrigues, D.S.; Buciumeanu, M.; Martinelli, A.E.; Nascimento, R.M.; Henriques, B.; Silva, F.S.; Souza, J.C.M. Mechanical Strength and Wear of Dental Glass-Ionomer and Resin Composites Affected by Porosity and Chemical Composition. *J. Bio-Tribo-Corros.* **2015**, *1*, 24. [[CrossRef](#)]
27. Fabris, D.; Souza, J.C.M.; Silva, F.S.; Fredel, M.; Mesquita-Guimarães, J.; Zhang, Y.; Henriques, B. Thermal residual stresses in bilayered, trilayered and graded dental ceramics. *Ceram. Int.* **2017**, *43*, 3670–3678. [[CrossRef](#)]
28. Denry, I.; Kelly, J.R. Emerging ceramic-based materials for dentistry. *J. Dent. Res.* **2014**, *93*, 1235–1242. [[CrossRef](#)]

29. Fabris, D.; Souza, J.C.M.; Silva, F.S.; Fredel, M.; Gasik, M.; Henriques, B. Influence of specimens' geometry and materials on the thermal stresses in dental restorative materials during thermal cycling. *J. Dent.* **2018**, *69*, 41–48. [[CrossRef](#)]
30. Sailer, I.; Makarov, N.A.; Thoma, D.S.; Zwahlen, M.; Pjetursson, B.E. All-ceramic or metal-ceramic tooth-supported fixed dental prostheses (FDPs)? A systematic review of the survival and complication rates. Part I: Single crowns (SCs). *Dent. Mater.* **2015**, *31*, 603–623. [[CrossRef](#)]
31. Souza, J.C.M.; Bentes, A.C.; Reis, K.; Gavinha, S.; Buciumeanu, M.; Henriques, B.; Silva, F.S.; Gomes, J.R. Abrasive and sliding wear of resin composites for dental restorations. *Tribol. Int.* **2016**, *102*, 154–160. [[CrossRef](#)]
32. Zhu, Y.; Zhu, R.; Ma, J.; Weng, Z.; Wang, Y.; Shi, X.; Li, Y.; Yan, X.; Dong, Z.; Xu, J.; et al. In vitro cell proliferation evaluation of porous nano-zirconia scaffolds with different porosity for bone tissue engineering. *Biomed. Mater.* **2015**, *10*, 55009. [[CrossRef](#)] [[PubMed](#)]
33. GARVIE, R.C.; HANNINK, R.H.; PASCOE, R.T. Ceramic steel? *Nature* **1975**, *258*, 703–704. [[CrossRef](#)]
34. Zhang, Y.; Lawn, B.R. Novel Zirconia Materials in Dentistry. *J. Dent. Res.* **2018**, *97*, 140–147. [[CrossRef](#)]
35. Schünemann, F.H.; Galárraga-Vinueza, M.E.; Magini, R.; Fredel, M.; Silva, F.; Souza, J.C.M.; Zhang, Y.; Henriques, B. Zirconia surface modifications for implant dentistry. *Mater. Sci. Eng. C* **2019**, *98*, 1294–1305. [[CrossRef](#)] [[PubMed](#)]
36. Roedel, S.; Souza, J.C.M.; Silva, F.S.; Mesquita-Guimarães, J.; Fredel, M.C.; Henriques, B. Optimized route for the production of zirconia structures with controlled surface porosity for biomedical applications. *Ceram. Int.* **2018**, *44*, 12496–12503. [[CrossRef](#)]
37. Fabris, D.; Souza, J.C.M.; Silva, F.S.; Fredel, M.; Mesquita-Guimarães, J.; Zhang, Y.; Henriques, B. The bending stress distribution in bilayered and graded zirconia-based dental ceramics. *Ceram. Int.* **2016**, *42*, 11025–11031. [[CrossRef](#)] [[PubMed](#)]
38. Galarraga-Vinueza, M.E.; Mesquita-Guimarães, J.; Magini, R.S.; Souza, J.C.M.; Fredel, M.C.; Boccaccini, A.R. Anti-biofilm properties of bioactive glasses embedding organic active compounds. *J. Biomed. Mater. Res. Part A* **2016**, *105*, 672–679. [[CrossRef](#)]
39. Galarraga-Vinueza, M.E.M.E.; Mesquita-Guimarães, J.; Magini, R.S.; Souza, J.C.M.J.C.M.; Fredel, M.C.M.C.; Boccaccini, A.R.A.R.; Magini, R.; Souza, J.C.M.J.C.M.; Fredel, M.C.M.C.; Boccaccini, A.R.A.R. Mesoporous bioactive glass embedding propolis and cranberry antibiofilm compounds. *J. Biomed. Mater. Res. Part A* **2018**, *106*, 1614–1625. [[CrossRef](#)]
40. Shao, R.-X.; Quan, R.-F.; Huang, X.-L.; Wang, T.; Xie, S.-J.; Gao, H.-H.; Wei, X.-C.; Yang, D.-S. Evaluation of porous gradient hydroxyapatite/zirconia composites for repair of lumbar vertebra defect in dogs. *J. Biomater. Appl.* **2016**, *30*, 1312–1321. [[CrossRef](#)] [[PubMed](#)]
41. Kim, H.-W.; Kim, H.-E.; Salih, V.; Knowles, J.C. Dissolution control and cellular responses of calcium phosphate coatings on zirconia porous scaffold. *J. Biomed. Mater. Res. A* **2004**, *68*, 522–530. [[CrossRef](#)] [[PubMed](#)]
42. Peñarrieta-Juanito, G.M.; Costa, M.; Cruz, M.; Miranda, G.; Henriques, B.; Marques, J.; Magini, R.; Mata, A.; Caramês, J.; Silva, F.; et al. Bioactivity of novel functionally structured titanium-ceramic composites in contact with human osteoblasts. *J. Biomed. Mater. Res. Part A* **2018**, *106*, 1923–1931. [[CrossRef](#)] [[PubMed](#)]
43. da Cruz, M.; Marques, J.; Peñarrieta-Juanito, G.; Costa, M.; Souza, J.; Magini, R.; Miranda, G.; Silva, F.; Duarte Sola Pereira da Mata, A.; Mendez Caramês, J. Hard and Soft Tissue Cell Behavior on Polyetheretherketone, Zirconia, and Titanium Implant Materials. *Int. J. Oral Maxillofac. Implants* **2019**, *34*, 39–46. [[CrossRef](#)] [[PubMed](#)]
44. Bosshardt, D.D.; Bornstein, M.M.; Carrel, J.-P.; Buser, D.; Bernard, J.-P. Maxillary sinus grafting with a synthetic, nanocrystalline hydroxyapatite-silica gel in humans: Histologic and histomorphometric results. *Int. J. Periodontics Restor. Dent.* **2014**, *34*, 259–267. [[CrossRef](#)]
45. Jensen, S.S.; Bornstein, M.M.; Dard, M.; Bosshardt, D.D.; Buser, D. Comparative study of biphasic calcium phosphates with different HA/TCP ratios in mandibular bone defects. A long-term histomorphometric study in minipigs. *J. Biomed. Mater. Res. B Appl. Biomater.* **2009**, *90*, 171–181. [[CrossRef](#)] [[PubMed](#)]
46. Bosshardt, D.D.; Chappuis, V.; Buser, D. Osseointegration of titanium, titanium alloy and zirconia dental implants: Current knowledge and open questions. *Periodontology 2000* **2017**, *73*, 22–40. [[CrossRef](#)]
47. Souza, J.C.M.; Sordi, M.B.; Kanazawa, M.; Ravindran, S.; Henriques, B.; Silva, F.S.; Aparicio, C.; Cooper, L.F. Nano-scale modification of titanium implant surfaces to enhance osseointegration. *Acta Biomater.* **2019**, *94*, 112–131. [[CrossRef](#)] [[PubMed](#)]
48. Lopes-Rocha, L.; Ribeiro-Gonçalves, L.; Henriques, B.; Özcan, M.; Tiritan, M.E.; Souza, J.C.M. An integrative review on the toxicity of Bisphenol A (BPA) released from resin composites used in dentistry. *J. Biomed. Mater. Res. B Appl. Biomater.* **2021**, *109*, 1942–1952. [[CrossRef](#)] [[PubMed](#)]
49. Tafur-Zelada, C.M.; Carvalho, O.; Silva, F.S.; Henriques, B.; Özcan, M.; Souza, J.C.M. The influence of zirconia veneer thickness on the degree of conversion of resin-matrix cements: An integrative review. *Clin. Oral Investig.* **2021**, *25*, 3395–3408. [[CrossRef](#)] [[PubMed](#)]
50. Messous, R.; Henriques, B.; Bousbaa, H.; Silva, F.S.; Teughels, W.; Souza, J.C.M. Cytotoxic effects of submicron- and nano-scale titanium debris released from dental implants: An integrative review. *Clin. Oral Investig.* **2021**, *25*, 1627–1640. [[CrossRef](#)] [[PubMed](#)]
51. Faria, M.; Guedes, A.; Rompante, P.; Carvalho, O.; Silva, F.; Henriques, B.; Özcan, M.; Souza, J.C.M. Wear Pathways of Tooth Occlusal Fissure Sealants: An Integrative Review. *Biotribology* **2021**, *27*, 100190. [[CrossRef](#)]
52. Souza, J.C.M.; Fernandes, V.; Correia, A.; Miller, P.; Carvalho, O.; Silva, F.; Özcan, M.; Henriques, B. Surface modification of glass fiber-reinforced composite posts to enhance their bond strength to resin-matrix cements: An integrative review. *Clin. Oral Investig.* **2022**, *26*, 95–107. [[CrossRef](#)] [[PubMed](#)]

53. Souza, J.C.M.; Pinho, S.S.; Braz, M.P.; Silva, F.S.; Henriques, B. Carbon fiber-reinforced PEEK in implant dentistry: A scoping review on the finite element method. *Comput. Methods Biomech. Biomed. Eng.* **2021**, *24*, 1355–1367. [[CrossRef](#)] [[PubMed](#)]
54. Ferreira, I.C.; Faria, M.; Torres, O.; Rompante, P.; Henriques, B.; Silva, F.; Özcan, M.; Souza, J.C.M. Damage of Dental Amalgam and Resin-Matrix Composite Surfaces After Exposure to Bleaching Agents: An Integrative Review. *J. Bio-Tribo-Corros.* **2021**, *7*, 118. [[CrossRef](#)]
55. Sanon, C.; Chevalier, J.; Douillard, T.; Kohal, R.J.; Coelho, P.G.; Hjerpe, J.; Silva, N.R.F.A. Low temperature degradation and reliability of one-piece ceramic oral implants with a porous surface. *Dent. Mater.* **2013**, *29*, 389–397. [[CrossRef](#)] [[PubMed](#)]
56. Song, Y.-G.; Cho, I.-H. Characteristics and osteogenic effect of zirconia porous scaffold coated with beta-TCP/HA. *J. Adv. Prosthodont.* **2014**, *6*, 285–294. [[CrossRef](#)] [[PubMed](#)]
57. Malmstrom, J.; Slotte, C.; Adolfsson, E.; Norderyd, O.; Thomsen, P. Bone response to free form-fabricated hydroxyapatite and zirconia scaffolds: A histological study in the human maxilla. *Clin. Oral Implants Res.* **2009**, *20*, 379–385. [[CrossRef](#)]
58. Teimouri, A.; Ebrahimi, R.; Emadi, R.; Beni, B.H.; Chermahini, A.N. Nano-composite of silk fibroin-chitosan/Nano ZrO<sub>2</sub> for tissue engineering applications: Fabrication and morphology. *Int. J. Biol. Macromol.* **2015**, *76*, 292–302. [[CrossRef](#)] [[PubMed](#)]
59. Mesquita-Guimarães, J.; Detsch, R.; Ramos, L.; Grünewald, A.; Henriques, B.; Fredel, M.C.; Silva, F.S.; Boccaccini, A.R. Evaluation of in vitro properties of 3D micro-macro porous bioactive hybrid scaffolds for bone grafting by human osteoblast-like cell growth. *J. Eur. Ceram. Soc.* **2019**, *39*, 2545–2558. [[CrossRef](#)]
60. Madeira, S.; Mesquita-Guimarães, J.; Ribeiro, P.; Fredel, M.; Souza, J.C.M.; Soares, D.; Silva, F.S.; Henriques, B. Y-TZP/porcelain graded dental restorations design for improved damping behavior—A study on damping capacity and dynamic Young's modulus. *J. Mech. Behav. Biomed. Mater.* **2019**, *96*, 219–226. [[CrossRef](#)]
61. Fabris, D.; Moura, J.P.A.; Fredel, M.C.; Souza, J.C.M.; Silva, F.S.; Henriques, B. Biomechanical analyses of one-piece dental implants composed of titanium, zirconia, PEEK, CFR-PEEK, or GFR-PEEK: Stresses, strains, and bone remodeling prediction by the finite element method. *J. Biomed. Mater. Res. B Appl. Biomater.* **2022**, *110*, 79–88. [[CrossRef](#)] [[PubMed](#)]
62. Askari, E.; Cengiz, I.F.; Alves, J.L.; Henriques, B.; Flores, P.; Fredel, M.C.; Reis, R.L.; Oliveira, J.M.; Silva, F.S.; Mesquita-Guimarães, J. Micro-CT based finite element modelling and experimental characterization of the compressive mechanical properties of 3-D zirconia scaffolds for bone tissue engineering. *J. Mech. Behav. Biomed. Mater.* **2020**, *102*, 103516. [[CrossRef](#)] [[PubMed](#)]
63. Balagangadharan, K.; Viji Chandran, S.; Arumugam, B.; Saravanan, S.; Devanand Venkatasubbu, G.; Selvamurugan, N. Chitosan/nano-hydroxyapatite/nano-zirconium dioxide scaffolds with miR-590-5p for bone regeneration. *Int. J. Biol. Macromol.* **2018**, *111*, 953–958. [[CrossRef](#)] [[PubMed](#)]